Bifunctional Au-Fe_3O_4 Nanoparticles for Protein Separation

Jie Bao,[†] Wei Chen,[†] Taotao Liu,[‡] Yulin Zhu,[†] Peiyuan Jin,[†] Leyu Wang,[†] Junfeng Liu,[†] Yongge Wei,[†] and Yadong Li[†,*]

[†]Department of Chemistry and [‡]Department of Biological Sciences and Biotechnology, Tsinghua University, Beijing 100084, P. R. China

ABSTRACT In this article, we report the synthesis of bifunctional Au-Fe_3O_4 nanoparticles that are formed by chemical bond linkage. Due to the introduction of Au nanoparticles, the resulting bifunctional Au-Fe_3O_4 nanoparticles can be easily modified with other functional molecules to realize various nanobiotechnological separations and detections. Here, as an example, we demonstrate that as-prepared Au-Fe_3O_4 nanoparticles can be modified with nitrilotriacetic acid molecules through Au–S interaction and used to separate proteins simply with the assistance of a magnet. Bradford protein assay and sodium dodecyl sulfate–polyacrylamide gel electrophoresis were performed to examine the validity of the separation procedure, and the phosphate determination method suggested that the as-separated protein maintained catalytic activity. This result shows the efficiency of such a material in protein separation and suggests that its use can be extended to magnetic separation of other biosubstances. Moreover, this synthetic strategy paves the way for facile preparation of diverse bifunctional and even multifunctional nanomaterials.

KEYWORDS: bifunctional nanoparticles · magnetic nanomaterials · protein separation

Based on the rapid development of their controlled synthesis, assembly, and modification, nanomaterials have been proved promising in a wide range of biotechnological applications, especially as highly sensitive and selective sensors and separators.[1–3] Among them, gold nanoparticles have been widely used in extremely sensitive biodetection for DNA and proteins. This is not only because their facile and robust interaction with thiol and disulfide groups enables functionalization of gold particles with various molecules which are capable of specifically recognizing biological substances, but also due to their exceptional optical properties that are influenced remarkably by their chemical environment, their agglomeration, their kinds, or even their conformational differences.[1,4–11] Meanwhile, magnetic nanoparticles are also attractive and strong candidates for applications such as diagnosis, therapeutics, separations, and magnetic resonance imaging for detections.[12] Some important progress in cancer diagnosis, protein separation, and detection has been made based on well-synthesized and functionalized iron oxide nanoparticles.[13–17]

As a form of bifunctional nanomaterials, nanoparticles combining gold and iron oxides inherit from the two components excellent surface chemistry, special optical properties, and superparamagnetic properties, all of which would greatly enhance the potential and broaden the application of such composite bifunctional nanomaterials. As a result, successful strategies for the synthesis of bifunctional gold−iron oxide nanoparticles are recognized as one of the major advances in nanobiotechnology.[18] Current successful synthetic protocols for such bifunctional nanomaterials include, for example, reducing Au^{3+} onto Fe_3O_4 nanoparticle surfaces *via* iterative hydroxylamine seeding, decomposing $Fe(CO)_5$ on the surface of the Au nanoparticles followed by oxidation in 1-octadecene solvent, and Au^{3+} reduction onto Fe_3O_4 nanoparticles deposited on silica cores to form a three-layer composite nanoparticle.[18–20]

Here, we report our recent success in the synthesis of bifunctional Au-Fe_3O_4 nanoparticles that are formed by simply linking two separately prepared nanomaterials by chemical bonds, rather than using chemical deposition processes. Compared to the Fe_3O_4 nanoparticles (4–20 nm) being used in the fabrication of dumbbell-like nanoparticles,[20] the particles we used were larger. As a result, stronger magnetic force, sufficient for the separation of bigger molecules, can be achieved. In order to prove their practicability and great potential in bioapplications, we further demonstrate the validity of such material for protein separation. The result showed that not only was highly efficient separation of the targeted protein obtained, but the as-separated

*Address correspondence to ydli@tsinghua.edu.cn.

Received for review August 24, 2007 and accepted October 10, 2007.

Published online October 31, 2007.
10.1021/nn700189h CCC: $37.00

protein also maintained catalytic activity. The success of our experiment indicates that the diversity of bifunctional Au-Fe_3O_4 nanomaterials can be realized by chemically linking various Au and Fe_3O_4 nanomaterials synthesized separately. In a broader sense, various bifunctional or even multifunctional nanomaterials could be easily synthesized through the linkage of chemical bonds.

RESULTS AND DISCUSSION

Fe_3O_4 nanoparticles of different sizes have been prepared successfully by several methods. Some use $Fe(acac)_3$ as iron precursor with necessary surfactants,[21,22] while some find it possible to synthesize monodispersed Fe_3O_4 nanoparticles in aqueous solution without surfactant.[23] Here, the amino-functionalized Fe_3O_4 nanoparticles were prepared in the way we have reported previously[24] and were used without further modification. Because of the existence of 1,6-hexadiamine in the reaction system and the coordination of amino groups to Fe atoms, the Fe_3O_4 nanoparticles have some amino groups on their surfaces. In order to conjugate Au particles to them, we then modified the surfaces of Fe_3O_4 nanoparticles with cysteine molecules by the formation of amide bonds between the surface amino groups of Fe_3O_4 and the carboxylic groups of cysteine. So the Fe_3O_4 nanoparticles were functionalized by thiol groups on their surfaces. The Au nanoparticles were synthesized in aqueous solution through the reduction of $HAuCl_4$ by $NaBH_4$. The thiol-modified Fe_3O_4 particles were then mixed with Au particles under ultrasonic conditions, and the Au particles were conjugated to the Fe_3O_4 particles by the strong interaction between Au and the thiol group. This strategy is shown schematically in Figure 1A. After being vigorously washed, the product was redispersed in ethanol. From Figure 1B, we can see clearly the color change of Fe_3O_4 nanoparticles before and after Au conjugation. The original color of Fe_3O_4 particles (0.2 mg/mL) is black, and that of Au (0.01 mg/mL) is red-purple, while the resulting bifunctional Au-Fe_3O_4 nanoparticles (0.2 mg/mL) turned to reddish brown. This suggests that the resulting Fe_3O_4-Au nanoparticles have inherited the colorimetric character of gold nanoparticles.

Magnetic measurements, which were taken at 298 K, showed that there is no significant change in the magnetic moment and coercivity of Fe_3O_4 nanoparticles before and after conjugation of Au particles. As shown in Figure 2A, the magnetization of Fe_3O_4 nanoparticles is about 58 emu/g, and that of Au-Fe_3O_4 nanoparticles is about 51 emu/g. The 12% decrease in magnetization suggests that the gold and cysteine molecules introduced to the original Fe_3O_4 nanoparticles were about 12% in weight. The coercivity of both materials can be found in the enlarged view of the central loop shown also in Figure 2A, 105 Oe for Fe_3O_4 and 95 Oe for Au-Fe_3O_4. Upon placement of a magnet

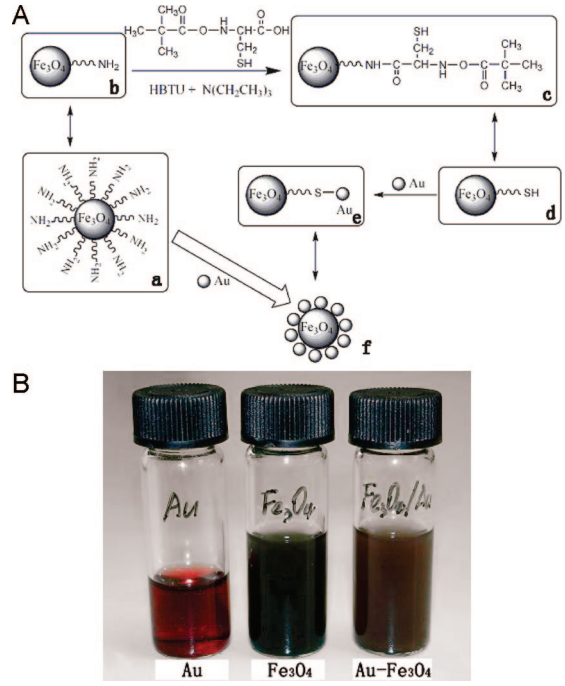

Figure 1. (A) Schematic illustration of bifunctional Au-Fe_3O_4 nanoparticle synthesis. Amino-functionalized Fe_3O_4 nanoparticles (a, simplified as b for the convenience of illustration) were first modified by Boc-L-cysteine to have surface thiol groups (c, simplified as d). Gold nanoparticles were the conjugated onto the surface of Fe_3O_4 nanoparticles to form the expected Fe_3O_4-Au bifunctional nanoparticles (f, simplified as e). (B) Color comparison of Au, Fe_3O_4, and Au-Fe_3O_4 nanoparticles.

besides the vials, both materials were quickly attracted to the walls of the vials within a few seconds, leaving the solution transparent, as shown in Figure 2B. The morphology of the product was characterized by transition electron microscopy (TEM) and scanning electron microscopy (SEM). From the images shown in Figure 3a,b, we can see that the 60 nm Fe_3O_4 particles are well surrounded by the 10 nm Au particles, and the ratio of Fe_3O_4 to Au nanoparticles is 10–15/1, based on estimation from Figure 3a. The high-resolution TEM images (Figure 3c) show that the Au particle and the Fe_3O_4 particle are in close contact with each other. Energy-dispersive analysis of X-rays (EDAX; Figure 3d) of selected areas of Au-conjugated Fe_3O_4 particles further reveals their elemental composition. Fe, Au, O, C, N, and S can all be easily found in the EDAX graph. Among those elements, Cu, C, and O are influenced by the copper grid, the carbon film, and their degree of oxidation. Fe and Au signals result from the Fe_3O_4 and Au particles which form the product, while N and S signals proved the existence of amino groups and cysteine molecules that function as Au immobilizer. Control experiments, in which we mixed amino-functionalized Fe_3O_4 nanoparticles that were not modified with thiol groups with gold particles under the same conditions, showed that Fe_3O_4 nanoparticles without surface thiol groups do not form bifunctional Au-Fe_3O_4 nano -

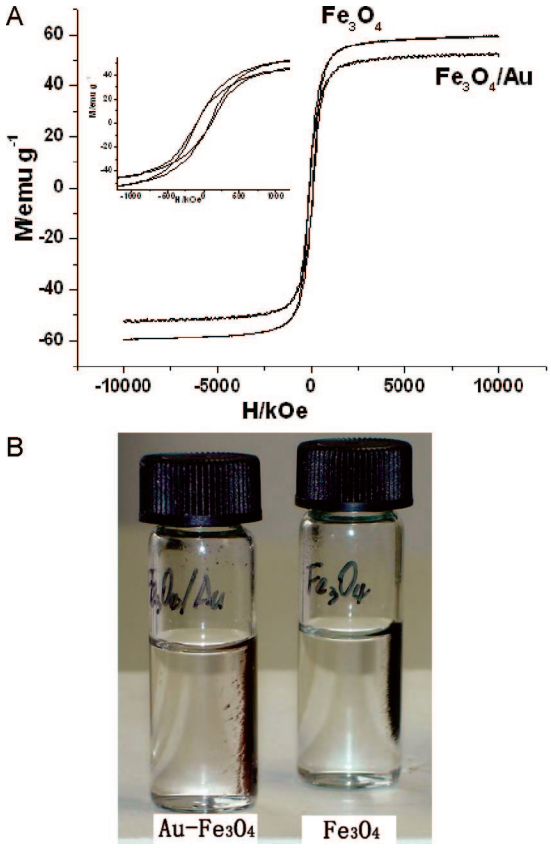

Figure 2. Magnetic property of bifunctional Au-Fe_3O_4 nanoparticles. (A) Magnetization curves of Fe_3O_4 and Au-Fe_3O_4 nanoparticles. (B) Both materials are attracted to the walls of the vial when a magnet is present.

particles. It proved that such a composite material is formed by Au−S bonds.

To use these materials for protein separation, we took advantage of the protocol of metal chelate affinity chromatography (MCAC).[25] We connected nickel ion (Ni^{2+})-coordinated *N*-[*N*α,*N*α-bis(carboxymethyl)-L-lysine]-16-mercaptohexadecanamide to the unoccupied binding sites of Au particles of the bifuncational nanoparticles using the strong Au−S interaction. The nickel ions (Ni^{2+}) can then attach to the six consecutive histidine residues (6xHis). Any protein (in this case arginine kinase (AK), ~43 kD) that is modified with 6xHis by genetic engineering would be easily separated in this way.

The separately collected imidazole wash buffer solutions were used in the following tests to confirm the existence of protein. The Bradford protein assay protocol (Coomassie Blue G-250)[26] was used as an instant method to examine for the existence of protein in those wash buffers. If a certain wash buffer contains proteins, it will turn the originally brown Coomassie Blue G-250 solution into a blue color, while wash buffer without protein in it will leave Coomassie Blue G-250 brown. As shown in Figure 4A, sample 1 is the last portion of wash buffer which was used to remove unbound protein residual. It contained no protein since the color of

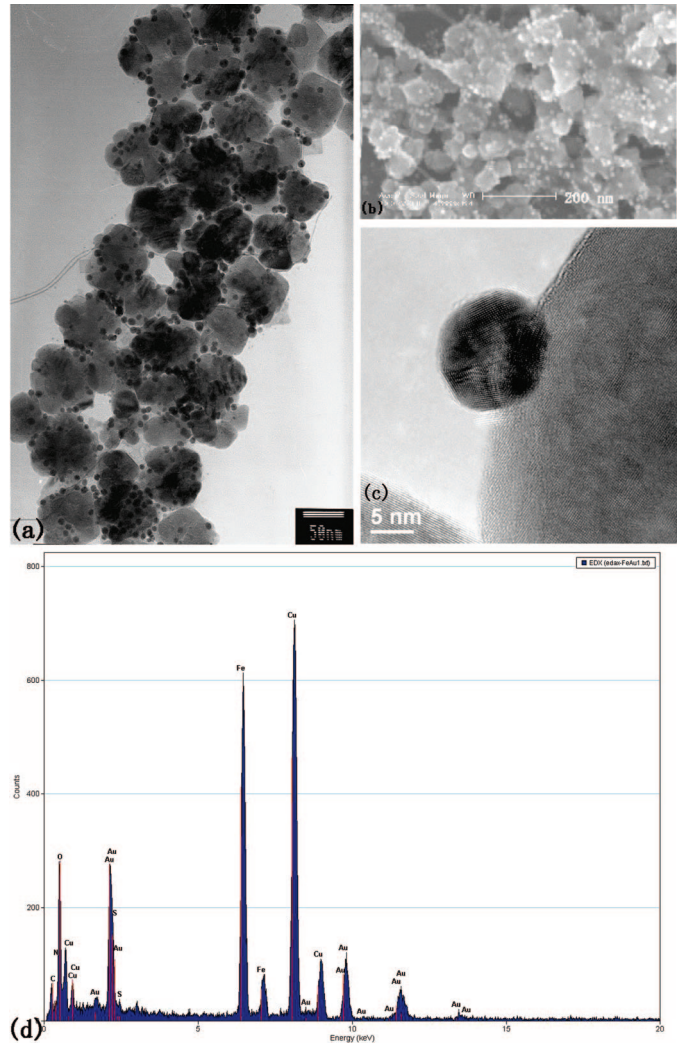

Figure 3. Characterization of bifunctional Au-Fe_3O_4 nanoparticles: (a,b) TEM images, (c) SEM image, (d) HRTEM image, and (e) EDAX.

Coomassie Blue solution remained brown. Sample 2 is 10 mM imidazole wash buffer which was used to release the bound proteins. It changed the color only slightly. Sample 3 is 500 mM imidazole wash buffer. It released bound proteins effectively since it turned the solution into blue. Comparison between samples 2 and 3 shows that sample 2 contained much fewer proteins than sample 3, which suggests that protein was bound firmly thus not easy to lose. Sample 3 also released bound proteins thoroughly since, immediately after we washed it again with 500 mM imidazole wash buffer (sample 4), no more protein was found to be released. By comparing samples 2 and 3 to samples 2* and 3*, whose color did not change after 10 and 500 mM imidazole buffer was added, respectively, we confirmed the existence of protein in the wash buffer of samples 2 and 3.

Sodium docecyl sulfate−polyacrylamide gel electrophoresis was then applied according to the literature[28] to examine the purity of the separated protein. As shown in Figure 4B, compared to the marker in lane 0, the original protein mixture solution (as shown in lane

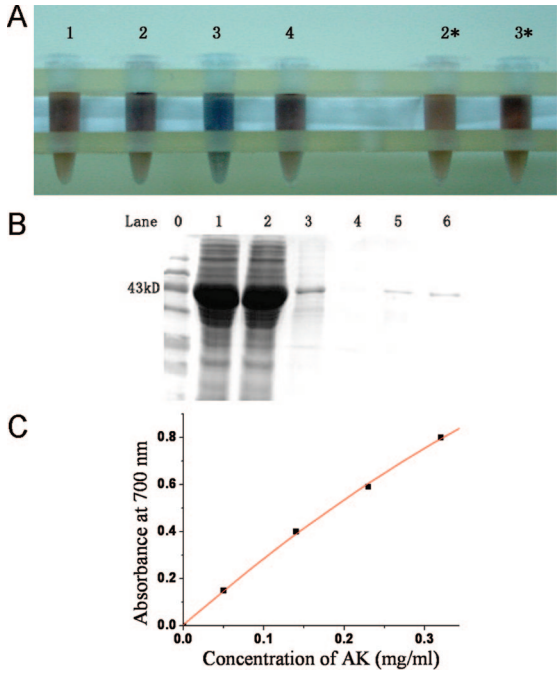

Figure 4. (A) Bradford protein assay of the separation efficiency: 1, the last portion of residual wash buffer, maintained the Coomassie Blue G-250 solution a brown color, contained no protein; 2, 10 mM imidazole wash buffer, turned the color slightly to blue, (compared with 2*, in which 10 mM imidazole buffer solution without protein was added), contained a few proteins; 3, 500 mM imidazole wash buffer, turned blue (compared with 3*, in which 500 mM imidazole buffer solution without protein was added), contained proteins; 4, 500 mM imidazole wash buffer added again, solution remained brown, no protein. (B) SDS−PAGE analysis of the separated protein: lane 0, marker; lane 1, original protein mixture solution; lane 2, protein mixture solution after separation; lane 3, first residual wash buffer; lane 4, last residual wash buffer; lane 5, 10 mM imidazole wash buffer; lane 6, 500 mM imidazole wash buffer. (C) Standard curve of absorbance *versus* AK concentration.

1) contained proteins of various molecular sizes. As the amount of the target protein to be separated exceeds the amount that could be held by those bifunctional nanoparticles during the separation process, there are still various proteins in the solution after some of them have been separated (as shown in lane 2). The nanoparticles holding proteins on their surfaces were first washed with buffer solution a few times so that no nonspecifically bound proteins remained (as shown in lanes 3 and 4 for comparison between the first and the last time of washing). The nanoparticles were then washed by 10 and 500 mM imidazole buffer solutions to dissociate the target protein. As shown in lanes 5 and 6, 43 kD AK of high purity was effectively separated and collected.

In order to test the practicability of using Au-conjugated Fe_3O_4 particles to separate protein, we further examined the activity of the separated AK in catalyzing the magnesium-dependent reversible phosphorylation of L-arginine by adenosine triphosphate. We chose to use the phosphate determination method based on an ascorbic acid-reduced ternary heteropolyacid system to examine the protein catalytic activity.[26,27] The blue ternary heteropolyacid was composed of bismuth, molybdate, and phosphate. Phosphate was released from *N*-phospho-L-arginine, which was formed during a certain period in the catalytic reaction. Standard AK of known concentration was used for L-arginine phosphorylation, and the absorbance of ternary heteropolyacid formed during the following reduction reaction at 700 nm was measured to give a standard curve of absorbance *versus* AK concentration (as shown in Figure 4C). The separated AK sample was then taken for phosphate determination, and the resulting absorbance was 0.15, suggesting that the separated AK sample maintained as much activity as that of 0.05 mg/mL standard AK. Assuming the separated protein maintains 100% activity, the loading capacity of the nanoparticles used in this experiment was 0.05 mg of protein per 1 mg of nanoparticles.

The bifunctional Au-Fe_3O_4 nanoparticles will not be destroyed by the separation process and can be reused readily. However, the loading capacity would decrease, and that is where further efforts should be made.

CONCLUSION

In this paper, we reported the synthesis of bifunctional Au-Fe_3O_4 nanoparticles and their use in separating protein which maintained high catalytic activity after being separated. The as-prepared bifunctional nanoparticles combined the merits of both gold and Fe_3O_4 nanoparticles and were formed by chemical bond linkage. Possessing around 12% gold by weight, the resulting bifunctional nanoparticles maintain excellent magnetic properties. Additionally, the ease of functionalizing them further facilitates wide and effective applications of this nanomaterial in various biological separations and detections. Furthermore, this experiment also suggested a new way to synthesize various bifunctional or multifunctional composite nanomaterials through simply linking two or several kinds of nanomaterials by chemical bonds.

METHODS

General Information. All chemicals were of analytical grade and used as received without further purification. Deionized water was used throughout. Chemicals for the synthesis of *N*-[*N*α,*N*α-Bis(carboxymethyl)-L-lysine]-16-mercaptohexadecanamide and for the preparation of protein mixture solution were purchased from Sigma-Aldrich or Alfa-Aesar. Other chemicals were all supplied by the Beijing Chemical Reagent Co. The TEM images were taken by using a Hitachi model H-800 transmission electron microscope with a tungsten filament at an accelerating voltage of

200 kV. The morphology of Au-Fe_3O_4 nanoparticles was further characterized by using a JSM-6301F scanning electron microscope. High-resolution transmission electron microscopy (HR-TEM) and energy-dispersive X-ray analysis spectroscopy (EDAX) were performed on a Tecnai F20 HRTEM. Magnetic measurements were carried out on a Lakeshore-7307 vibrating sampling magnetometer. The UV−vis absorption in the protein catalytic activity assay was measured with a Specord 200 UV−vis analytic spectrophotometer (Jena, Germany).

Preparation of Bifunctional Au-Fe_3O_4 Nanoparticles. A mixture of 1.0 g of $FeCl_3 \cdot 6H_2O$, 2.0 g of anhydrous sodium acetate, and 6.0 g of 1,6-hexadiamine in 30 mL of glycol was heated at 200 °C for 6 h to give Fe_3O_4 nanoparticles (Supporting Information, Figure S1). In a 5 mL dimethylformamide (DMF) solution of 0.1 g of dispersed Fe_3O_4 nanoparticles were dissolved 0.1 g of Boc-L-cysteine and 0.18 g of *O*-benzotriazole-*N*,*N*,*N*′,*N*′-tetramethyluroniumhexafluorophosphate (HBTU). Then, 0.9 mL of triethylamine was added at drop speed under vigorous stirring, and the mixture was allowed to react overnight. The product was separated magnetically and washed with DMF (5 mL × 2) and water (5 mL × 2). Au nanoparticles were synthesized following the report[28] by Jana *et al*., with some modifications. First, we mixed 5 mL of 0.5 mmol/L $HAuCl_4$ aqueous solution with 5 mL of 0.2 mol/L cetyltrimethylammonium bromide (CTAB). Next, 0.6 mL of 0.01 mol/L $NaBH_4$ was added, and the solution was stirred to react for 5 min and allowed to settle overnight. Then, 1.0 mg of Fe_3O_4 nanoparticles, prepared as described above, were dispersed in 3 mL of ethanol and added dropwise into a 10 mL aqueous solution of Au particles under ultrasonic condition. After a further 5 min of reaction, the reddish-brown Au-Fe_3O_4 nanoparticles were separated magnetically and washed with ethanol to remove the unbound Au particles.

Preparation of Nitrilotriacetic Acid (NTA)-Modified Au-Fe_3O_4 Nanoparticles. Au-Fe_3O_4 nanoparticles (1.0 mg; the average number of gold nanoparticles per Fe_3O_4 nanoparticle is around 15) were dispersed in 5 mL of ethanol and mixed with 0.6 mg of *N*-[*N*α,*N*α-bis(carboxymethyl)-L-lysine]-16-mercaptohexadecanamide, which was synthesized according to the literature[29] (Supporting Information, Figures S2−S4), in 1 mL of acetone. After the reaction mixture was stirred for 12 h, the product was separated magnetically and washed with deionized water three times. The particles were then mixed with 10 mL of 100 mM $NiCl_2$ aqueous solution and allowed to react for 30 min for the coordination of Ni^{2+} ions to NTA molecules. They were then washed with deionized water three times to remove extra nickel ions. The final product was redispersed in 10 mL of Tris−HAc buffer solution (20 mM Tris−HAc, pH 8.10) and stored for later use.

Arginine Kinase Separation Using Au-Fe_3O_4 Nanoparticles. NTA-modified Au-Fe_3O_4 nanoparticles (1.0 mg) were dispersed in 1 mL of cell lysate from which had been removed cell debris by centrifugal separation. [The cells were *Escherichia coli* cells which had been transfected with plasmid encoding arginin kinase modified with six consecutive histidines (6xHis-AK) and induced by isopropyl β-D-thiogalactoside (IPTG) for high AK expression. The lysate was obtained by sonication.] After the reaction mixture was shaken for 5 min, the Au-Fe_3O_4 nanoparticles were separated using a magnet and washed several times with Tris−HAc buffer solution to remove the residual protein solution and nonspecifically bound proteins on the surface of nanoparticles until the wash buffer contained no protein. Next, 10 and 500 mM imidazole buffer solutions, which are capable of dissociating proteins from the nanoparticles, were added in turn to wash the 6xHis-AK-bound Au-Fe_3O_4 particles, and the wash buffers were collected separately.

Analysis of Separated Protein. Bradford protein assay was performed according to the literature as an instant detection method.[30] The denaturing polyacrylamide gel electrophoresis (SDS−PAGE) was performed as reported[31] for each sample to examine the purity of the separated protein. For protein catalytic activity assay, we used the phosphate determination method and followed the procedures as reported.[26,27]

Acknowledgment. This work was supported by NSFC (90406003, 20401010), the Specialized Research Fund for the Doctoral Program of Higher Education, the Foundation for the Author of National Excellent Doctoral Dissertation of P. R. China, and the State Key Project of Fundamental Research for Nanomaterials and Nanostructures (2003CB716901).

Supporting Information Available: XRD analysis of Fe_3O_4 nanoparticles used in this research, synthetic scheme of *N*-[*N*α,*N*α-bis(carboxymethyl)-L-lysine]-16-mercaptohexadecanamide, and NMR and MS analysis of the products. This material is available free of charge *via* the Internet at http://pubs.acs.org.

REFERENCES AND NOTES

1. Elghanian, R.; Storhoff, J. J.; Mucic, R. C.; Letsinger, R. L.; Mirkin, C. A. Selective Colorimetric Detection of Polynucleotides Based on the Distance-Dependent Optical Properties of Gold Nanoparticles. *Science* **1997**, *277*, 1078–1081.
2. Cui, Y.; Wei, Q.; Park, H.; Lieber, C. M. Nanowire Nanosensors for Highly Sensitive and Selective Detection of Biological and Chemical Species. *Science* **2001**, *293*, 1289–1292.
3. Gu, H.; Xu, K. M.; Xu, C. J.; Xu, B. Biofunctional magnetic nanoparticles for protein separation and pathogen detection. *Chem. Commun.* **2006**, *941*, 949.
4. Love, J. C.; Estroff, L. A.; Kriebel, J. K.; Nuzzo, R. G.; Whitesides, G. M. Self-Assembled Monolayers of Thiolates on Metals as a Form of Nanotechnology. *Chem. Rev.* **2005**, *105*, 1103–1170.
5. Daniel, M. C.; Astruc, D. Gold Nanoparticles: Assembly, Supramolecular Chemistry, Quantum-Size-Related Properties, and Applications toward Biology, Catalysis, and Nanotechnology. *Chem. Rev.* **2004**, *104*, 293–346.
6. Taton, T. A.; Mirkin, C. A.; Letsinger, R. L. Scanometric DNA Array Detection with Nanoparticle Probes. *Science* **2000**, *289*, 1757–1760.
7. Cao, Y. C.; Jin, R.; Mirkin, C. A. Nanoparticles with Raman Spectroscopic Fingerprints for DNA and RNA Detection. *Science* **2002**, *297*, 1536–1540.
8. Nam, J. M.; Thaxton, C. S.; Mirkin, C. A. Nanoparticle-Based Bio-Bar Codes for the Ultrasensitive Detection of Proteins. *Science* **2003**, *301*, 1884–1886.
9. Storhoff, J. J.; Elghanian, R.; Mucic, R. C.; Mirkin, C. A.; Letsinger, R. L. One-Pot Colorimetric Differentiation of Polynucleotides with Single Base Imperfections Using Gold Nanoparticle Probes. *J. Am. Chem. Soc.* **1998**, *120*, 1959–1964.
10. Fu, A.; Micheel, C. M.; Cha, J.; Chang, H.; Yang, H.; Alivisatos, A. P. Discrete Nanostructures of Quantum Dots/Au with DNA. *J. Am. Chem. Soc.* **2004**, *126*, 10832–10833.
11. Chah, S.; Hammond, M. R.; Zare, R. N. Gold Nanoparticles as a Colorimetric Sensor for Protein Conformational Changes. *Chem. Biol.* **2005**, *12*, 323–328.
12. Penn, S. G.; He, L.; Natan, M. Nanoparticles for bioanalysis. *Curr. Opin. Chem. Biol.* **2003**, *7*, 609–615.
13. Jun, Y. W.; Huh, Y. M.; Choi, J. S.; Lee, J. H.; Song, H. T.; Kim, S.; Yoon, S.; Kim, K. S.; Shin, J. S.; Suh, J. S.; Cheon, J. Nanoscale Size Effect of Magnetic Nanocrystals and Their Utilization for Cancer Diagnosis via Magnetic Resonance Imaging. *J. Am. Chem. Soc.* **2005**, *127*, 5732–5733.
14. Song, H. T.; Choi, J. S.; Huh, Y. M.; Kim, S.; Jun, Y. W.; Suh, J. S.; Cheon, J. Surface Modulation of Magnetic Nanocrystals in the Development of Highly Efficient Magnetic Resonance Probes for Intracellular Labeling. *J. Am. Chem. Soc.* **2005**, *127*, 9992–9993.
15. Huh, Y. M.; Jun, Y. W.; Song, H. T.; Kim, S.; Choi, J. S.; Lee, J. H.; Yoon, S.; Kim, K. S.; Shin, J. S.; Suh, J. S.; Cheon, J. In Vivo Magnetic Resonance Detection of Cancer by Using Multifunctional Magnetic Nanocrystals. *J. Am. Chem. Soc.* **2005**, *127*, 12387–12391.
16. Xu, C. J.; Xu, K. M.; Gu, H. W.; Zheng, R. K.; Liu, H.; Zhang, X. X.; Guo, Z. H.; Xu, B. Dopamine as A Robust Anchor to Immobilize Functional Molecules on the Iron Oxide Shell of Magnetic Nanoparticles. *J. Am. Chem. Soc.* **2004**, *126*, 9938–9939.

17. Won, J.; Kim, M.; Yi, Y. W.; Kim, Y. H.; Jung, N.; Kim, T. K. A Magnetic Nanoprobe Technology for Detecting Molecular Interactions in Live Cells. *Science* **2005**, *309*, 121–125.
18. Stoeva, S. I.; Huo, F.; Lee, J. S.; Mirkin, C. A. Three-Layer Composite Magnetic Nanoparticle Probes for DNA. *J. Am. Chem. Soc.* **2005**, *127*, 15362–15363.
19. Lyon, J. L.; Fleming, D. A.; Stone, M. B.; Schiffer, P.; Williams, M. E. Synthesis of Fe Oxide Core/Au Shell Nanoparticles by Iterative Hydroxylamine Seeding. *Nano Lett.* **2004**, *4*, 719–723.
20. Yu, H.; Chen, M.; Rice, P. M.; Wang, S. X.; White, R. L.; Sun, S. H. Dumbbell-like Bifunctional Au-Fe_3O_4 Nanoparticles. *Nano Lett.* **2005**, *5*, 379–382.
21. Sun, S. H.; Zeng, H. Size-Controlled Synthesis of Magnetite Nanoparticles. *J. Am. Chem. Soc.* **2002**, *124*, 8204–8205.
22. Sun, S. H.; Zeng, H.; Robinson, D. B.; Raoux, S.; Rice, P. M.; Wang, S. X.; Li, G. X. Monodisperse MFe_2O_4 (M = Fe, Co, Mn) Nanoparticles. *J. Am. Chem. Soc.* **2004**, *126*, 273–279.
23. Kang, Y. S.; Risbud, S.; Rabolt, J. F.; Stroeve, P. Synthesis and Characterization of Nanometer-Size Fe_3O_4 and γ-Fe_2O_3 Particles. *Chem. Mater.* **1996**, *8*, 2209–2211.
24. Wang, L. Y.; Bao, J.; Wang, L.; Zhang, F.; Li, Y. D. One-Pot Synthesis and Bioapplication of Amine-Functionalized Magnetite Nanoparticles and Hollow Nanospheres. *Chem. Eur. J.* **2006**, *12*, 6341–6347.
25. Petty, K. J. In *Current Protocols in Molecular Biology*; Ausubel, F. M., Brent, R., Kingston, R. E., Moore, D. D., Seidman, J. G., Smith, J. A., Petty, K. J., Eds.; John Wiley & Sons: New York, 1996; pp 10.11.10–10.11.24.
26. Virden, B. R.; Watts, D. C.; Baldwin, E. Adenosine 5′-triphosphate-arginine phosphotransferase from lobster muscle: purification and properties. *Biochem. J.* **1965**, *94*, 536–544.
27. Chen, B. Y.; Guo, Q.; Cuo, Z.; Wang, X. C. Improved activity assay method for Arginine Kinase based on a ternary heteropolyacid system. *Tsinghua Sci. Technol.* **2003**, *4*, 422–427.
28. Jana, N. R.; Gearheart, L.; Murphy, C. J. Wet Chemical Synthesis of High Aspect Ratio Cylindrical Gold Nanorods. *J. Phys. Chem. B* **2001**, *105*, 4065–4067.
29. Xu, C. J.; Xu, K. M.; Gu, H. W.; Zhong, X. F.; Guo, Z. H.; Zheng, R. K.; Zhang, X. X.; Xu, B. Nitrilotriacetic Acid-Modified Magnetic Nanoparticles as a General Agent to Bind Histidine-Tagged Proteins. *J. Am. Chem. Soc.* **2004**, *126*, 3392–3393.
30. Bradford, M. M. A rapid and sensitive method for the quantitation of microgram quantities of protein utilizing the principle of protein-dye binding. *Anal. Biochem.* **1976**, *72*, 248–254.
31. Laemmli, U. K. Cleavage of Structural Proteins during the Assembly of the Head of Bacteriophage T4. *Nature* **1970**, *227*, 680–685.